Bubble-free injection of liquid metal for the direct microfabrication of leaf-inspired 3D-topological conduit-networks and a flexible serpentine circuit with superior electrical resistance to aging

Cite as: AIP Advances **10**, 015226 (2020); https://doi.org/10.1063/1.5125178
Submitted: 22 October 2019 . Accepted: 20 December 2019 . Published Online: 21 January 2020

Yukai Zhang, Jiaqi Sun, Qingran Wang, Shiheng Chen, Lishuang Yao, Wei Rao, Jinguang Cai, and Wenming Wu

Bubble-free injection of liquid metal for the direct microfabrication of leaf-inspired 3D-topological conduit-networks and a flexible serpentine circuit with superior electrical resistance to aging

Cite as: AIP Advances 10, 015226 (2020); doi: 10.1063/1.5125178
Submitted: 22 October 2019 • Accepted: 20 December 2019 •
Published Online: 21 January 2020

Yukai Zhang,[1] Jiaqi Sun,[1,2] Qingran Wang,[1] Shiheng Chen,[1] Lishuang Yao,[1] Wei Rao,[3] Jinguang Cai,[4] and Wenming Wu[1,a)]

AFFILIATIONS

[1]State Key Laboratory of Applied Optics, Changchun Institute of Optics, Fine Mechanics and Physics, Chinese Academy of Sciences, Changchun 130033, China
[2]University of Chinese Academy of Sciences, Beijing 100000, China
[3]Technical Institute of Physics and Chemistry of the Chinese Academy of Sciences, Beijing 100000, China
[4]China Academy of Engineering Physics, Chengdu 610000, China

[a)]**Author to whom correspondence should be addressed:** wuwenming627@163.com

ABSTRACT

Flexible circuit boards are widely used in smart consumer electronic devices. In this paper, a novel methodology, which is different from the traditional etching and screen printing methods that generally rely on screen printed conductive ink as a conductor to form the required circuit in a dielectric film, has been reported. Liquid metal was directly injected into biocompatible polymer microchips, based on the air-diffusion mechanism, in order to prevent the circuit board from being directly exposed to the outside environment. The liquid metal circuit board that was produced had good thermal conductivity because the thermal conductivity of gallium is about 60 times that of water and 1000 times higher than that of air. In addition, the liquid metal circuit board has good ductility and repeatability, which is required to meet the extreme deformation that is experienced in most electrical applications. The proposed method has the ability to fabricate irregular circuit boards and complex patterns with channel-lengths as high as 4 m or channel-widths as small as 30 μm. This method can not only solve the problem of the traditional circuit boards being difficult to modify and repair, but it can also effectively protect the circuit and realize high fidelity of the circuit.

I. INTRODUCTION

Flexible printed circuits (FPCs)[1] are a type of very reliable and high quality circuit boards. Due to their high wiring density, light weight, thin construction, and good bending properties,[2–4] FPCs have become an indispensable component of intelligent consumer[5] electronics. FPCs are mainly used in small, portable, wearable devices,[6–10] such as smart watches, mobile phones, drones, PCs, and even automotive terminals. Currently, flexible circuits are electroplated onto flexible insulating substrates (such as polyamides and polyester films).[11]

Recently, a lot of interest has been paid to the direct injection of conductive liquid materials (such as silver nanowires,[12,13] copper nanowires,[11] silver inks, and liquid metals) into biocompatible protective materials such as polydimethylsiloxane[14] (PDMS) pipes. However, the process is complicated and when the circuit is bent repeatedly in use, problems such as work hardening of the metal plating can result in the occurrence of fatigue fracture.[15] Modifying or repairing the circuit is difficult, the heat flux of the plated metal is low, and the poor biological compatibility of the substrate are problems that are yet to be solved.[16] In addition, it is currently difficult to manufacture irregular patterns in a complex circuit.[3,8]

For these materials, metals that are liquid at room temperature can be injected, which have good ductility,[10] elasticity (with excellent recovery behavior), stability, and high conductivity values.

In addition, considering that liquid metals have a much higher thermal conductivity than that of water, air, and many nonmetallic media,[16–18] liquid metal circuit boards are able to achieve more efficient heat transfer and have a better heat dissipation capacity than traditional circuit boards.[19,20] In practical applications, gallium and its alloys stand out because they are far less toxic than other metals that could be used, such as mercury and silver nanowires. At the same time, because liquid metals have fluidity and plasticity similar to those of liquids,[21] circuit boards with complex structures of three-dimensional irregular patterns can be manufactured according to demand.

Microfluid injection has been proven to be a beneficial technique,[22,23] which is able to produce conductive patterns that have photolithographic resolution. However, the manufacturing process of this equipment is very complicated, and the heat dissipation of the circuit boards is poor, and it is difficult to produce complex circuits with irregular 3D figures.[24,25] Aqueous solutions usually exhibit Newtonian rheological behavior. However, liquid metals display inferior stress behavior due to the need to rupture the oxide film.[26]

At present, most of the filling methods have been concentrated in an aqueous solution.[23] Completing the filling of complex microchannels with liquid metal is a difficult problem. There are several differences between liquid metal solutions and aqueous solutions:

(1) The injection of metal requires a sufficient pressure differential to cause the oxide film to break and induce the metal to flow into the channel.
(2) Microfluidic channels with closed ends tend not to be filled during the process, and the air in the channels is easily compressed during injection.
(3) The channels limit the ability of the liquid metals to create dense and distinct channel structures during injection.
(4) The complex microfluidic structures usually require multiple exits and seals, which may cause uneven filling of the channels.
(5) The injection action of the injection pump creates a gap between the closed end of the channel and the corner, which prevents the liquid metal from fully filling the channel.

In order solve the aforementioned problems, a simple, fast, practical, and effective method to fabricate flexible circuit boards has been proposed in this paper. The surface modification of a PDMS chip with low adhesion (silica gel:coagulant = 10:1) was carried out using a plasma machine. This process improved the surface wettability of the PDMS, and the surface tension was also decreased.[16,22] As a result, it was easy for the liquid metal to enter the microchannel. The entire channel was smoothly filled with the application of a relatively low constant pressure[27] (about 50 kPa), and therefore, the problem of the liquid metal filling the microchannel has been solved by optimizing the operation. The liquid metal gallium alloy has high electrical conductivity and good thermal fatigue resistance. As a result, the problem of the low heat flux of traditional flexible circuit boards and fatigue fracture caused by repeated bending has been solved. This method solves several problems with filling channels with liquid metal that occurs in the previous approaches.[26]

II. EXPERIMENTS

A. Chip fabrication

In order to meet the requirements of different functional devices in practical applications, it is necessary to complete the filling of more subtle, complex, and irregularly patterned circuit boards. A high fidelity PDMS-PDMS leaf vein chip[28] was constructed, which was based on veins that occur in nature (Fig. 1) to ensure the irregular nature of the patterns as well as their complexity.

B. Experimental testing of repeated bending and recovery

On the basis of the theory of bending, three groups of experiments of bending and restoring of the flexible circuit board were carried out. Each test was performed with bending angles of 45°, 90°, and 120°. In the experiment, each circuit was bent 25 times to produce one data point, 1000 bending experiments were carried out, and the data were recorded by using an electrochemical analyzer.

In order to ensure the narrow structure of the channel, a 30 μm Y pattern was formed using a laser etching machine to fabricate the PDMS-PDMS chip. A liquid metal circuit board with dimensions of 0.5 m–1.5 m was selected for use. It was completely filled, and a Dry Thermostat GL-150B was used to heat the liquid metal circuit board. The temperature was increased from 30 °C to 85 °C, with

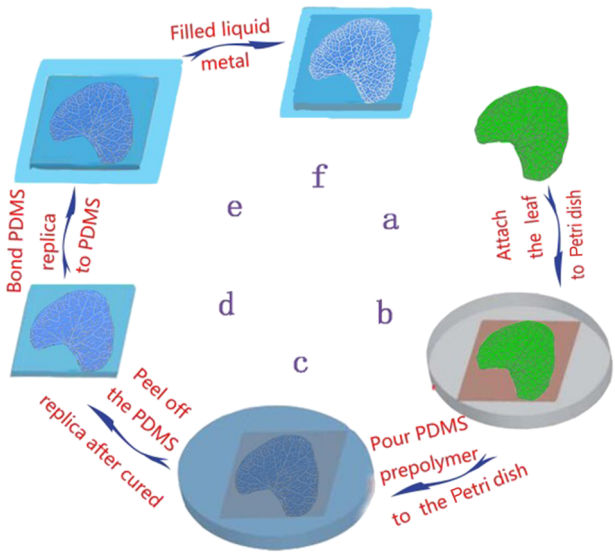

FIG. 1. The fabrication steps of a leaf-inspired complex circuit board by direct replication of the microvascular networks from natural leaves into a microfluidic PDMS device. The natural leaf (a) attached to single-sided tape (b) is mounted onto a Petri dish (d) using a double sided tape (c). The PDMS prepolymer is poured over the leaf and cured (e) before the PDMS replica is removed. An enclosed microchannel is formed by sealing the PDMS replica with a glass or PDMS substrate after treating it with oxygen plasma (f). The biomimetic chip is placed in an oven at 80 °C for 2 h in order to stabilize the bonding strength. (f) Filling the vane pipe with the liquid metal using negative pressure.

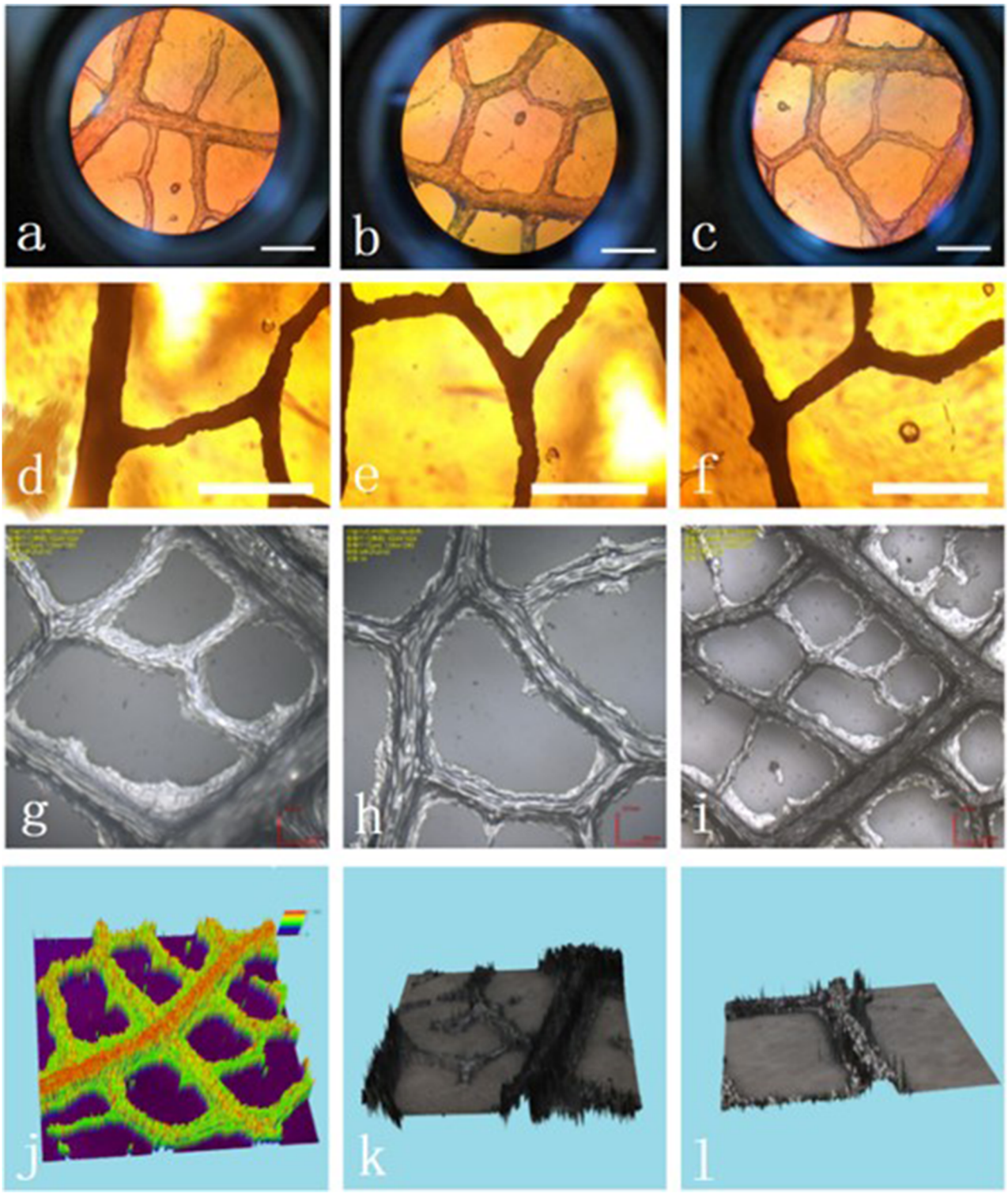

FIG. 2. [(a)–(f)] Micrographs of PDMS-PDMS veins filled with the liquid metal using a fluorescence microscope. [(g)–(i)] The morphology of PDMS-PDMS vanes filled with anterior and empty tubes using a confocal microscope. [(j)–(l)] Using a confocal microscope to observe the stereosection of the branch vein filled with the PDMS-PDMS leaf vein in the front and the empty pipeline. The scale bars are 100 μm.

a 5 °C step. The electrochemical analyzer was used to record the changes of the resistance values of the metal circuits at each temperature step. The graph of the change in the resistance of the circuit board with the increase in temperature has shown that the resistance values of the metal circuits varied less with temperature.

C. Testing the tensile resistance

A fully filled, 2-m long highly complex liquid metal circuit was selected for this test, and a JF-100P microcomputer tensile testing machine was used to stretch the flexible circuit board. The resistance was measured by the electrochemical analyzer, and the value of its resistance before stretching was 77.08 Ω. The stretching process was that the liquid metal flexible circuit board was stretched horizontally to 105% of its original length and the corresponding resistance value was recorded after it was stretched to 125% of its original length. The circuit was then returned to its original size, and the resistance values were measured at 125% and 115% of its original length. After many measurements, the error bars were formed by integrating the measured experimental data.

D. Repeated stretching experiment

In order to characterize the stability of the flexible liquid metal circuit board, the flexible circuit board was repeatedly stretched to 120% of its original length. In the experiment, the resistance was measured every 25 stretches, and 1000 stretching experiments were carried out, and the data were recorded by the electrochemical analyzer. After being stretched a 1000 times, the resistance value of the board changed from 77.92 Ω to 80.51 Ω and the resistance value changed by 3.329%. The results showed that the flexible circuit board had strong stability, and furthermore, it could be used in the production of a practical circuit board.

E. Liquid injection

The leaf template that was used in this experiment was from the Glechomahederacea plant, which has a six-level branch vein, and the smallest branch vein has a width of about 30 μm (Fig. 2). In order to ensure the narrow structure of the channel, a channel with a width of 40 μm was etched in the circuit board using a laser etching machine, in order to fabricate the PDMS-PDMS chip. At a certain pressure (about 50 kPa), the microchannel was completely filled using a syringe, and it demonstrated that a much more complex (highly irregular, subtle, 3D) structure could be produced when the pressure was high enough and that liquid metals can fully fill the closed ends and corners of the microchannel, including the ability to produce dense metal patterns in closed 3D pipes. The liquid metal could fully fill structures as small as several micrometers and up to a few meters long. Thus, the highly irregular three-dimensional pattern of a flexible liquid metal circuit board was realized.

F. Confocal microscopy

The analysis of the positive leaves and the negative PDMS copies was performed with an OLS4000 3D laser microscope (scanning mode: XYZ fine scanning color, image size: 1024 × 1024, image size (μm): 1284 × 1280, objective MPLFLN10: zoom X). It was shown that the blade structure was three-dimensional and the figure's height was irregular. The relationship of the relative size between the main vein and the branch vein has been given, and the finest filled vein was about 20 μm wide.

G. Bending and recovery experiment of the liquid metal circuit board at different angles

The snake-shaped liquid metal circuit board was tested with a self-made bending instrument. The resistance of the material was measured using an electrochemical analyzer, and the resistance value prior to bending was 37.15 Ω. The bending process is as follows: the flexible circuit board was bent to an angle of 20°, 40°, 60°, 80°, 100°, and 120°. It was then returned in the opposite direction of the original path, that is, bent to an angle of 120°, 100°, 80°, 60°, 40°, and 20°, and then returned to the original state. At the same time, the resistance values of each position were recorded, and the process diagram of the change in the resistance, shown in Fig. 5(e), was integrated into four sets of experimental data to form an error line.

H. Bending experiment of the liquid metal circuit board at different curvature radii

We measured the relationship among the equivalent radius, the flexible circuit, and resistivity. The resistance of the material was measured using an electrochemical analyzer. A Teflon tube of 1 m long, 0.3 mm inner diameter, and 0.6 mm outer diameter was wound on a 6.6 mm, 16.6 mm, and 35.5 mm diameter cylinder. It was filled with gallium-*indium* alloy with a 2.5 ml syringe. Under the changing voltage of 0 V–1 V, the voltage-current diagram can be drawn and the value of resistance can be calculated by the formula. It was found that in the case of the same bending deformation, the smaller the equivalent radius, the greater the corresponding resistivity.

III. RESULT AND DISCUSSION

A. Effect of the surface tension of the liquid metal on the filling process

First of all, by measuring the contact angle of the liquid metal at different melting points (>90°, Fig. 3), it has been shown that the degree of wetting of the liquid metal was less than that of an aqueous solution, that is, it had a high surface tension. This has shown that the resistance of the liquid metal in the pipeline was greater than that of the aqueous solution. Therefore, the degree of wetting was low and was limited by the surface and the template, and therefore, it could not realize the arbitrary mode filling and it is difficult to inject[26] (for example, being injected into a microfluidic channel and a hollow wire). This resulted in low efficiency and low completion of the filling of the flexible circuit boards with the liquid metal, resulting in most of the liquid metal being wasted in the filling process.

B. Optimization for complete filling of the closed ends and corners of the microchannels

The flow of liquid metals in microchannels has been discussed in this section by comparing the different velocities of PMMA and PDMS microfluid pipes with the change in pressure [Figs. 4(a) and 4(b)]. A physical image was taken of the magnified microstructure of PMMA and PDMS microchannels filled with the liquid metal (gallium alloy) at pressures of 170 kPa and 60 kPa, respectively

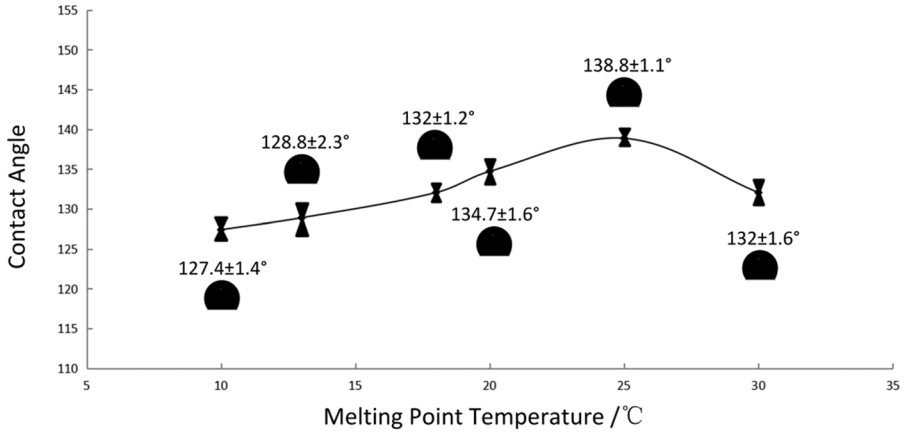

FIG. 3. Contact angle measurement of the liquid metal with a melting point of 10° C, 13° C, 18° C, 20° C, 25° C, and 30° C with a room temperature of 30° C.

[Fig. 4(c)]. It can be seen from the diagram that when the pressure was high enough (usually greater than atmospheric pressure), the liquid metal was able to completely fill the closed end and corner of the microchannel.

The experimental results showed that, as long as the pressure was stable and high enough, the liquid metal could completely fill the closed snake-shaped micropipeline for a length of 230 μm up to 4 m, no matter what the permeability of the material was (PDMS or

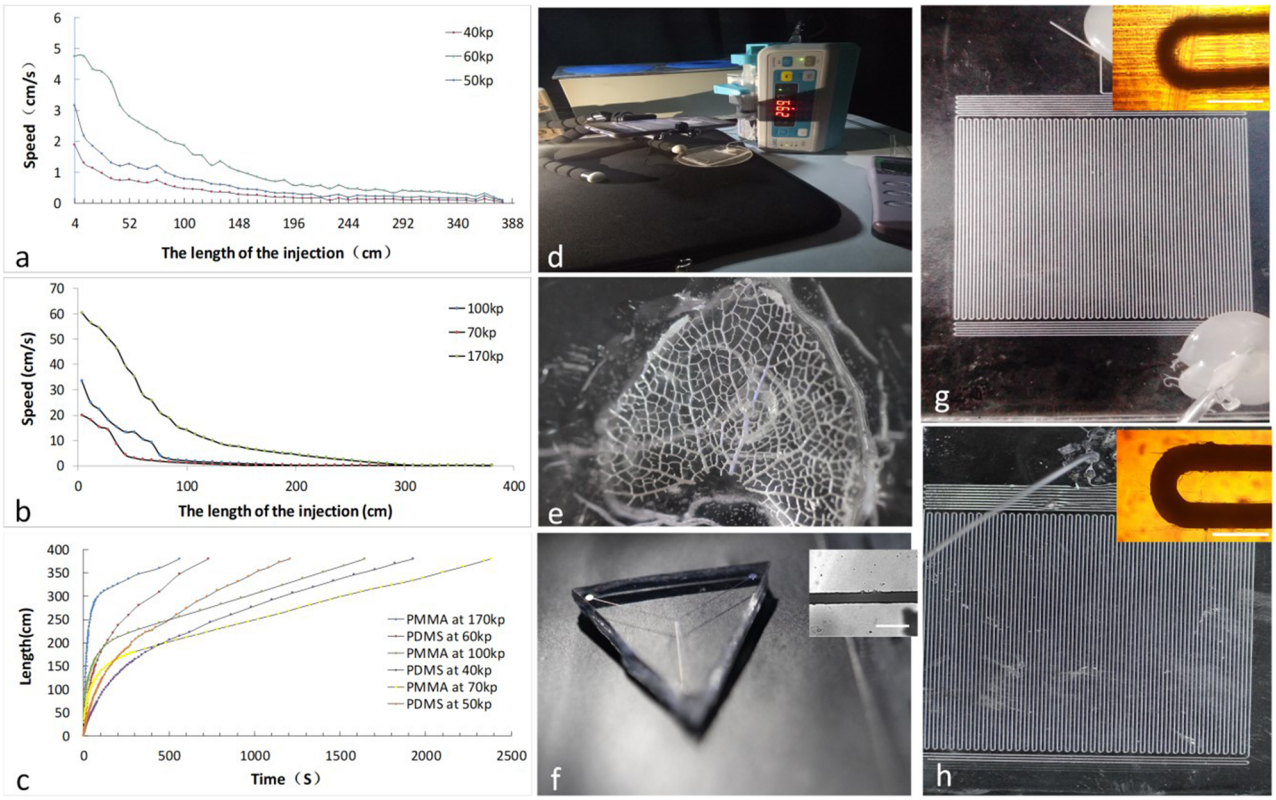

FIG. 4. The liquid metal injected into the different shapes of the microchannels. (a) Velocity of the liquid metal during injection into PDMS-PDMS microtubes under pressures of 40 kp, 50 kp, and 60 kp-injection length diagram. (b) Relationship between injection speed and injection length by injection of the liquid metal into PMMA-PMMA microtubes under pressures of 70 kp, 100 kp, and 170 kp. (c) Injection length-time diagrams of PMMA-PMMA microtubes and PDMS-PDMS microtubes filled at 170 ka and 60 ka, respectively. (d) Microtube filling liquid metal circuit board physical diagram. (e) Y-type PDMS-PDMS microtubes (30 μm wide), fully filled with the liquid metal. (f) PDMS-PDMS veins fully filled with the liquid metal. (g) PMMA-PMMA microtubes filled with the liquid metal, whole and local microcosmic physical drawings. (h) PDMS-PDMS microtubes completely filled with liquid metal, whole and local microphysical drawings.

TABLE I. E-modulus of PDMS templates with different amounts of crosslinking agents.

	Crosslinker:monomer ratios		
	1:10(RSD, %)	1:15(RSD, %)	1:20(RSD, %)
E-modulus (N mm^{-2})	1.1(2.1%)	0.6(0.8%)	0.1(1.2%)

PMMA). Thus, the problem of uneven closure and corners in the filling process has been solved.

C. Optimization of the monomer ratio of the crosslinking agent

In order to ensure that the flexible metal circuit board has better bending ability as well as repeatability and to make sure that the

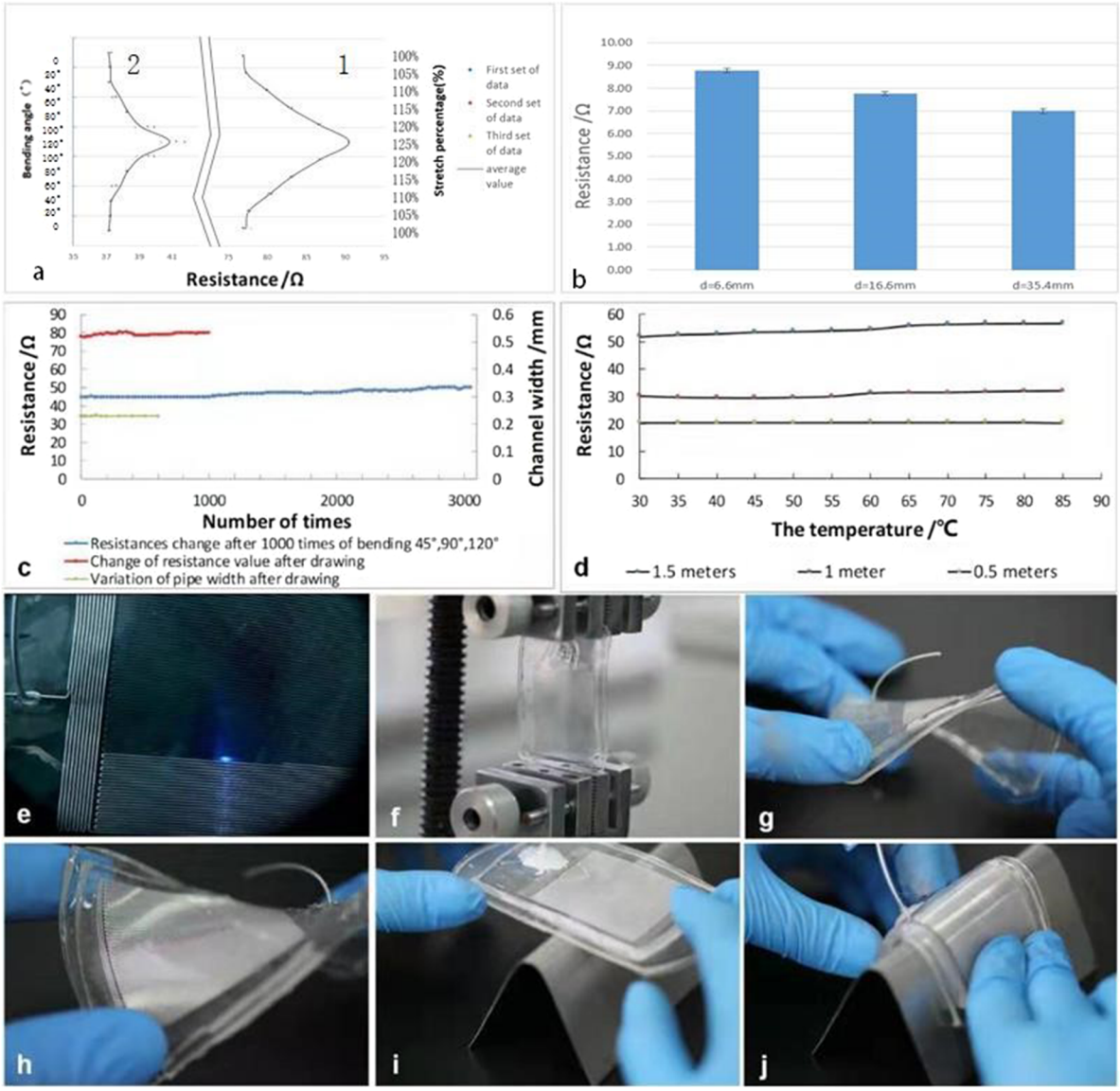

FIG. 5. (a) 1. The tensile resistance of 2 m long PDMS-PDMS microtubes in a fully filled PDMS-PDMS microtube. 2. The bending resistance of a 1 m long pipe in a fully filled PDMS-PDMS microtube for different degrees of bending. (b) Resistance change diagram of metal filled 1-m-long Teflon tube with an inner diameter of 0.3 mm under different curvature radii. (c) The tensile bending resistance of the sample is measured from the changes of the pipe width and resistance. (d) The resistance-temperature diagram of 0.5 m, 1 m, and 1.28 m long pipes filled with PDMS-PDMS microtubes at different temperatures. (e) The process diagram of liquid metal filled PDMS-PDMS serpentine microtubule. (f) Drawing process of PDMS-PDMS microtubes fully filled with the liquid metal. [(g) and (h)] Reverse operation of completely filled PDMS-PDMS microtubules with the liquid metal. [(i) and (j)] The snake-shaped liquid metal circuit board was tested with a self-made bending instrument.

filling process was not easily split with increased pressure, a preliminary optimization of the ratio of the crosslinking agent and the monomer in the manufacture of the PDMS polymer pipe was performed. PDMS was used with a crosslinking agent and a monomer ratio of 1:5, 1:10, 1:15, and 1:20. It was found from the experiment that the sealing strength of the 1:5 PDMS could not meet the requirement, and the close sealing between the PDMS-PDMS could not be realized by the manual plasma cleaning machine (KT-S2DQX).

PDMS with a ratio of 1:20 had very high viscosity, which could easily lead to the destruction of the fine pipeline; therefore,, none of them will be used. Compared with PDMS with ratios of 1:10 and 1:15, it was found that the pipe made of 1:10 PDMS had greater elasticity and less deformation, so a PDMS-PDMS pipe with a ratio of 1:10 was chosen (Table I).

D. The influence of external conditions on the flexible liquid metal circuit board's electrical properties

The electrical properties and stability of the liquid metal flexible circuit board were investigated by changing the bending degree, elongation, stretching and bending times, and the temperature of the liquid metal flexible circuit board. The stability of the liquid metal circuit board was studied using the variation of the resistance at different tensile lengths [Fig. 5(a–1)], bending angles [Fig. 5(a–2)], and curvature radii [Fig. 5(b)]. It is worth noting that the rate of change of the resistance of the liquid metal circuit board was less than 1.5% in both the beginning and end states of the experiment. The variation of the resistance value [Fig. 5(c), blue] and the measurement of the pipeline width indirectly show the resistance change [Fig. 5(c), green] after the different times of the stretch recovery after 1000° of bending of the 1.28 m long liquid metal circuit board have been listed. The use cycles and the degree of deformation of the liquid metal flexible circuit board were then studied. The experimental results have shown that the flexible circuit board can keep its performance relatively stable over more cycles of use, and the snake-shaped pipe counteracts the effect of some of the deformation. Heat treatment [Fig. 5(d)] of the liquid metal circuit boards with different lengths was carried out in order to study the change of the resistance at different temperatures. In this work, it was found that the thermal conductivity of the liquid metal circuit board was very good due to the strong thermal conductivity of the gallium itself, which greatly reduces the thermal effect in the operation of the circuit board. It was found that the longer the length of the liquid metal circuit board, the greater the volatility of the resistance with the increase in temperature. It is speculated that this phenomenon is related to the thermal conductivity of the outer PDMS material.

IV. CONCLUSION

The strategy of increasing the pressure in order to encapsulate the microfluidic structure and realize the fabrication of an arbitrary 3D flexible liquid metal circuit board with high resolution, high efficiency, and high degree of sealing has been proposed in this paper. The circuit board that was prepared using this method had good electrical conductivity and good thermal conductivity, as well as good recovery, stability, and ductility, and was able to prevent the circuit from being destroyed. After many cycles of bending, stretching, and heating processes, the change in electrical conductivity was very small, which means it could be used in electronic components. Liquid metal circuit boards are used for highly scalable circuits, such as vane electrodes and motion sensors. Due to its good biological compatibility, it could greatly promote the development of wearable devices and flexible displays.

Compared with the vacuum filling method of the liquid metal,[26] the filling method that has been proposed in this paper has greatly improved the maneuverability of the process for mass production on the basis of complete filling, and it has reduced the cost for actual industrial production. Compared with a printable metal-polymer conductor,[16] herein the filling accuracy of the circuit board and the fabrication of a 3D liquid metal circuit board with irregular and complex microstructures have been improved. The proposed process has solved the problem that a flexible circuit board cannot currently be modified and repaired and that it is difficult to make a circuit with a complex irregular figure. The further refinement of the circuit board and the creation of more complex flexible circuit boards will provide a more extensive application opportunity for the development of flexible circuit boards.

ACKNOWLEDGMENTS

This project was supported by the CAS Pioneer Hundred Talents Program, the National Natural Science Foundation of China (Grant No. 61704169), the Natural Science Foundation of Jilin Province (Grant No. 20180520112JH), and the Talent Project of Jilin Province.

REFERENCES

[1] J. Wang, G. Cai, S. Li, D. Gao, J. Xiong, and P. S. Lee, Adv. Mater. **30**, 1706157 (2018).
[2] X.-S. Li, X.-Z. Xiang, L. Wang, and X.-J. Bai, Rare Met. **37**, 191–195 (2016).
[3] D. Brosteaux, A. Fabrice, M. Gonzalez, and J. Vanfleteren, IEEE Electron Device Lett. **28**, 552–554 (2007).
[4] A. C. Siegel, S. T. Phillips, M. D. Dickey, N. Lu, Z. Suo, and G. M. Whitesides, Adv. Funct. Mater. **20**, 28 (2010).
[5] A. Furniturewalla, M. Chan, J. Sui, K. Ahuja, and M. Javanmard, Microsyst. Nanoeng. **4**, 20 (2018).
[6] A. Wu, L. Wang, E. Jensen, R. Mathies, and B. Boser, Lab Chip **10**, 519–521 (2010).
[7] Y. G. Hu, T. Zhao, P. L. Zhu, Y. Zhang, X. W. Liang, R. Sun, and C. P. Wong, in *IEEE International Conference on Electronic Packaging Technology (ICEPT)* (IEEE, 2017), pp. 1361–1365.
[8] N. Matsuhisa, M. Kaltenbrunner, T. Yokota, H. Jinno, K. Kuribara, T. Sekitani, and T. Someya, Nat. Commun. **6**, 7461 (2015).
[9] V. K. Varadan, D. Hilbich, L. Shannon, and B. L. Gray, paper presented at the Nanosensors Biosensors, and Info-Tech Sensors and Systems, 2016, 2016.
[10] M. Kubo, X. Li, C. Kim, M. Hashimoto, B. J. Wiley, D. Ham, and G. M. Whitesides, Adv. Mater. **22**, 2749–2752 (2010).
[11] Y.-Y. Hsu, M. Gonzalez, F. Bossuyt, J. Vanfleteren, and I. De Wolf, IEEE Trans. Electron Devices **58**, 2680–2688 (2011).
[12] K. Wang, X. Yang, Z.-l. Li, H. Xie, Y.-z. Zhao, and Y.-h. Wang, Optoelectron. Lett. **14**, 195–199 (2018).
[13] N. Matsuhisa, D. Inoue, P. Zalar, H. Jin, Y. Matsuba, A. Itoh, T. Yokota, D. Hashizume, and T. Someya, Nat. Mater. **16**, 834–840 (2017).
[14] B. H. Jo, L. M. Van Lerberghe, K. M. Motsegood, and D. J. Beebe, J. Microelectromech. Syst. **9**, 76–81 (2000).
[15] M. Mosallaei, B. Khorramdel, M. Honkanen, P. Iso-Ketola, J. Vanhala, and M. Mantysalo, in *IEEE Microelectronics Packaging (NORDPAC)* (IEEE, 2017), pp. 78–83.
[16] L. Tang, S. Cheng, L. Zhang, H. Mi, L. Mou, S. Yang, Z. Huang, X. Shi, and X. Jiang, iScience **4**, 302–311 (2018).

[17]M. D. Dickey, ACS Appl. Mater. Interfaces **6**, 18369–18379 (2014).
[18]S. Zhu, J.-H. So, R. Mays, S. Desai, W. R. Barnes, B. Pourdeyhimi, and M. D. Dickey, Adv. Funct. Mater. **23**, 2308–2314 (2013).
[19]Y. Deng and J. Liu, Heat Mass Transfer **46**, 1327–1334 (2010).
[20]Z. Liu, *Electrically Conductive and Thermally Conductive Materials for Electronic Packaging* (State University of New York, Buffalo, 2005).
[21]T. Daeneke, K. Khoshmanesh, N. Mahmood, I. A. de Castro, D. Esrafilzadeh, S. J. Barrow, M. D. Dickey, and K. Kalantar-Zadeh, Chem. Soc. Rev. **47**, 4073–4111 (2018).
[22]B. L. Cumby, G. J. Hayes, M. D. Dickey, R. S. Justice, C. E. Tabor, and J. C. Heikenfeld, Appl. Phys. Lett. **101**, 174102 (2012).
[23]H. Song, Y. Wang, and K. Pant, Biomicrofluidics **5**, 24107 (2011).
[24]C. Chae, Y. H. Seo, Y. Jo, K. W. Kim, W. Song, K. S. An, S. Choi, Y. Choi, S. S. Lee, and S. Jeong, ACS Appl. Mater. Interfaces **7**, 4109–4117 (2015).
[25]F. Han, X. Su, M. Huang, J. Li, Y. Zhang, S. Zhao, F. Liu, B. Zhang, Y. Wang, G. Zhang, R. Sun, and C.-P. Wong, J. Mater. Chem. C **6**, 8135–8143 (2018).
[26]Y. Lin, O. Gordon, M. R. Khan, N. Vasquez, J. Genzer, and M. D. Dickey, Lab Chip **17**, 3043–3050 (2017).
[27]T. Jung and S. Yang, Sensors **15**, 11823–11835 (2015).
[28]W. Wu, R. M. Guijt, Y. E. Silina, M. Koch, and A. Manz, RSC Adv. **6**, 22469–22475 (2016).